Identification of relevant wavelet functions for multiscale characterization of manufactured surfaces using a genetically optimized neural network

Sabeur Mezghani[1]

Abstract
Multiscale surface characterization is a powerful tool that is used for process monitoring, surface quality control, and manufacturing optimization by establishing a link between process variables and functional performances. The multiscale decomposition approach using continuous and discrete wavelets is widely applied to take into account scales dependency. However, the optimal choice of the analysis wavelet function and the number of decomposition level is still a big issue. In this article, the artificial neural network theory was combined with the wavelet concept and was optimized based on the genetic algorithm to identify the relevant wavelet function for multiscale characterization of abraded surface topographies. Then, an extensive wavelet function library was developed and the proposed algorithm was applied to topographic data obtained from various abrasive finishing processes. The results show the pertinence of this approach to select the relevant wavelet, and a universal relevant wavelet function for abraded surface characterization was determined.

Keywords Wavelet neural network · Genetic optimization · Multiscale characterization · Surface roughness · Abrasive process

1 Introduction

Inspection of workpiece surface topographies is actually considered an effective strategy for manufacturing process monitoring [1–4] and product quality optimization and control [5–7]. However, topographic data usually contain process contributions at multiple scales because of different physical phenomena occurring during processing at different localizations in time, space, and frequency. Hence, the use of standard surface characterization methods (ISO 4287, ISO 13565, …) may lead to unreliable results due to data pre-filtering leading to a significant loss of information [8, 9]. Performances of surface diagnostic and discrimination are then greatly altered. To take into account such multiscale behavior, processing techniques that decompose the observed data at different scales are necessary [8]. Various harmonic and morphological approaches were proposed in the literature [10] such as pass band filtering, discrete [11, 12] and continuous [9, 13] wavelet decomposition, the evaluation length variations method [14, 15], and modal decomposition [16].

Among these approaches, wavelet decomposition is well suited to depicting surface features with local nonlinearities and fast variations, thanks to their intrinsic properties of finite support and self-similarity [17]. Further, it provides more flexibility and rapidity for dividing a given n-dimensional function (signal, image…) into multiple-scale components in comparison to other spectral techniques.

However, one of the major limitations is the difficulty of the choice of the optimal mother wavelet function and decomposition levels [18, 19]. In fact, this choice can influence the spatial and frequency resolution of the decomposition, which is directly proportional to the width of the used wavelet in the spatial and the Fourier space [20]. However, their impact on the quality of feature detection and approximation remains a controversial subject.

In fact, for example, in texture classification applications, some comparative studies conclude that the wavelet function selection is application dependent and has insignificant effects on the results in some applications [20]. However, in case of honed surface characterization, the influence of the choice of

✉ Sabeur Mezghani
sabeur.mezghani@ensam.eu

[1] Arts et Métiers ParisTech, MSMP-EA7350, Rue Saint Dominique, BP 508, 51006 Châlons-en-Champagne Cedex, France

the wavelet functions was demonstrated [18] by analyzing the capacity of a given wavelet function to detect typical honing features at the right spatial frequency of their apparitions. Further, the authors demonstrate that the regularity that is useful for getting nice features such as smoothness of the reconstructed signal or image is a fundamental property of the wavelet family for the topographic profile analysis goal. In another study, Bigerelle et al. show, by comparison of eight wavelet functions based on a statistical indicator, that the analysis of the topographic profile of abraded surfaces leads to the same spatial localization regardless of the parameters of the abrasive process and the wavelet shapes [19]. It appears from literature that there is not yet a universal methodology or criterion allowing the identification of relevant wavelet function, but it can be remarked that all approaches take into consideration the quality of data reconstruction from all its components. This reconstruction can be interpreted as an approximation problem of the considered data $f\left(\overrightarrow{x}\right)$ by the sum of its component $f_a\left(\overrightarrow{x}\right)$ at each scale a.

$$f\left(\overrightarrow{x}\right) = \tilde{f}\left(\overrightarrow{x}\right) + \varepsilon = \sum_{a_{min}}^{a_{max}} f_a\left(\overrightarrow{x}\right) + \varepsilon \quad (1)$$

where $\tilde{f}\left(\overrightarrow{x}\right)$ is the reconstructed signal or image from all its components $f_a\left(\overrightarrow{x}\right)$ from the lower scale a_{min} to the maximal scale a_{max} and ε is the target error of reconstruction.

Otherwise, many studies [21–23] have been reported on the ability of the wavelet neural networks (WNN) approach, proposed by Zhang and Benveniste [22], for solving the nonlinear function approximation problem that estimates an unknown function G that relies on the input data $\overrightarrow{x}$ to the output y by the following expression [21]:

$$y = G\left(\overrightarrow{x}\right) = F\left(\overrightarrow{x}, \psi_{a,b}, w\right) + \varepsilon \quad (2)$$

where ε is the target error.

A conventional WNN consists of a feed-forward neural network with one hidden layer and takes one or more inputs and the output layer that consists of one or more linear combiners or summers. It is based on the integration of two concepts: the wavelets and the neural networks by applying wavelet function ψ as activation function in every neuron in the hidden layer of the neuronal network [22, 23]. The number of hidden neurons that are not known in advance corresponds to the dilated and translated wavelets (from a single-wavelet function called mother wavelet) used in a WNN approximation model.

It is obvious that the most relevant mother wavelet function to represent given data is that which allows its reconstruction with a negligible target error ε and using the less complex wavelet basis (by dilatation and translation of the mother wavelet).

This article proposes a methodology based on the genetic algorithm (GA) optimized wavelet neural network to the identification of the pertinent wavelet function for multiscale characterization of manufactured surface topography. Then, the multiscale surface topography characterization using wavelet decomposition is first presented. Next, the proposed approach for relevant wavelet function selection is described. Finally, application of this method to topography profiles generated by various abrasive processes is performed and results are discussed.

2 Multiscale surface topography characterization

Here, we give a brief description of the wavelet-based multiscale surface characterization approach [24, 25]. Multiscale analysis of the surface texture allows determining a quantitative expression for the manufacturing impact on the surface. It involves the decomposition of its topographic profiles into different roughness scales.

This decomposition uses the continuous wavelet transform, which can be considered a mathematical microscope, where the resolutions are the basic functions obtained from a single wavelet or mother wavelet $\psi(x)$ by dilation (or compression) and translation [24]. The result of the decomposition makes it possible to identify the various scales of the topographic signal after a 1D inverse wavelet transformation [24, 25]. The inverse continuous wavelet transformation can be computed based on a discretized version of the single integral formula based on this decomposition [25]; the characterization methodology consists then of determining statistical parameters derived from ISO4287, ISO13565, or ISO12085 at each scale from the scales of waviness to roughness [24]. Then, a multiscale representation of the topographic profile that better reflects the variations in the process or the intended function of the component is obtained. Existing literatures in surface metrology show various purposes of the application of this approach such as process monitoring [11, 13, 24] and the identification of abrasive mechanisms activated during the finishing process [9, 14].

Figure 1 illustrates the influence of choosing the mother wavelet function on the scale and amplitude of the detected surface features. It shows a face-milled topographic profile (Fig. 1a), its decomposition into 32 scales by using various wavelet functions (Fig. 1b–d) and the determination of its *Mq* multiscale spectrum (the quadratic mean height average of surface irregularities at each scale) for each considered wavelet function (Fig. 1e). We can observe firstly that the multiscale wavelet decomposition separates surface components in different ways according to the type of wavelets (Fig. 1b–d).

Moreover, two peaks are observed in the Mq spectrum (Fig. 1e) independently of the used wavelet function. They indicate clearly and respectively the largest wavelength component of the topographic signal, i.e., the form component and the periodic surface feature which can be related to the feed rate variable of the turning operation.

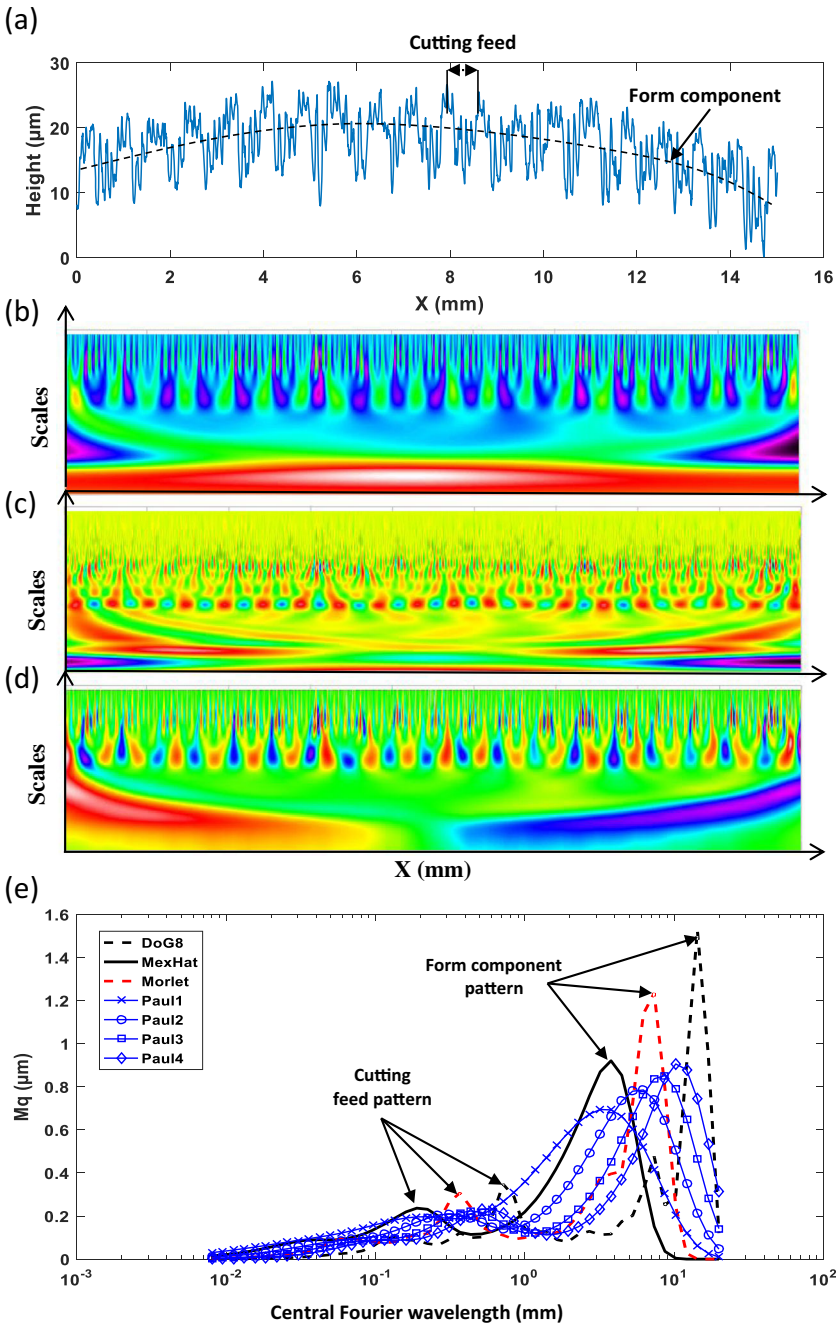

Fig. 1 Multiscale characterization of topographic profile of milled surface. **a** The topographic profile, examples of its multiscale decomposition using different wavelet functions. **b** Mexican hat also called DoG2 (second Gaussian derivative). **c** Morlet and **d** Paul2 (color scale is normalized in the range [0,1] for a better visual comparison). **e** The Multiscale Mq spectrum obtained based on various wavelet functions

Finally, it can be remarked that the detected peaks using Paul wavelet are right shifted toward higher wavelengths (lower frequencies) and become less skewed as order increases. Thus, Paul wavelets offer poorer frequency resolution and better spatial localization.

3 Methodology of relevant wavelet function selection

The proposed methodology consists of establishing a network regression model that mimics the multiscale surface topography characterization approach described in Sect. 2, that is, the direct wavelet transform followed by the inverse wavelet transform (Fig. 2). We exploit here the fact that for the continuous wavelet transform, the reconstructed profile can be obtained by just the sum of the real part of the wavelet transform over all scales due to the redundancy in time and scale as detailed in [26]. Then, the wavelet function in the regression network model substitutes the wavelet function of the direct wavelet transformation.

This regression network model is based on the GA-optimized WNN algorithm to adapt the wavelet basis to the training data. It is determined by pondering a set of wavelets

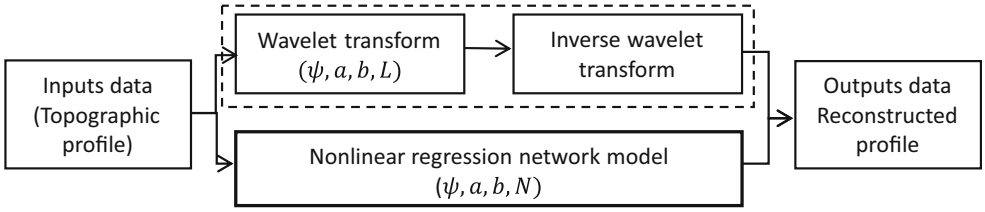

Fig. 2 Principle of the proposed wavelet selection approach (L and N are, respectively, the number of decomposition level and the number of hidden neurons; ψ is the wavelet function; a and b are, respectively, the scale and translation coefficient of each wavelet)

dilated and translated from one mother wavelet with weight values to approximate a given signal [27, 28].

3.1 Principle of WNN-optimized GA method

The general WNN structure relating the input data X (topographic profile data) to the output data Y (reconstructed profile data) is presented in Fig. 3. Note that in our case since we look to reconstructing exactly the analyzed profile, $X = Y$ and $n = m$.

The numbers of neurons in input and output layers are equal and depend on the profile length.

The weights $\omega_{i,\ k}$ and $\tilde{\omega}_{k,j}$ are optimized by the back-propagation algorithm until they reach the desired value of error criteria or the predefined number of iterations (epochs) [29].

To assess the quality of the developed model and the reconstructed profile, two error criteria comparing the input and output data of the WNN structure are considered here:

– The mean square error (MSE):

$$\mathrm{MSE} = \frac{1}{n}\sqrt{\sum_{i=1}^{n}(Y-X)^2} \tag{3}$$

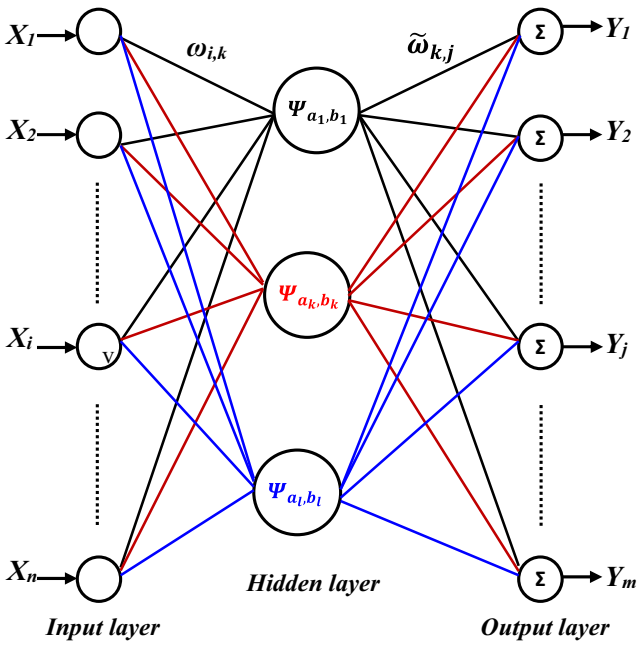

Fig. 3 The general structure of a wavelet neural network

– The correlation coefficient:

$$r = \frac{n\sum XY - (X)(\sum Y)}{\sqrt{n(\sum X^2) - (\sum X)^2}\sqrt{n(\sum Y^2) - (\sum Y)^2}} \tag{4}$$

X and Y are, respectively, the measured and predicted topographic profile by the developed model, and n is the number of the dataset.

The scale parameter a_k and translation parameter b_k of WNN allow wavelets to analyze signals in different scales and to access specific information. These two variables are initialized in a random manner [22, 23, 29]. GA evolves here, adjusts, and optimizes automatically the scale parameter a_k and translation parameter b_k of each hidden neuron of the WNN as proposed [29] until the end condition is satisfied. GA is a directed random search technique that is widely used in optimization problems where the number of parameters is large and the analytical solutions are difficult to obtain [30–32]. It uses the concept of the evolution mechanism (crossover and mutation) [32, 33], in which the genetic information changes for every generation, and the individuals who better adapt to their environment survive preferentially [31, 32].

The basic genetic algorithm is as follows [33]:

1. Create randomly an initial population of the two considered variable values (translation and dilatation coefficients of the wavelet mother function).
2. Evaluate all the individuals using an evaluation function.
3. Select a new population from the old population based on the fitness of the individuals as given by the evaluation function.
4. Apply mutation and crossover genetic operators to members of the population to create new solutions.
5. Evaluate these newly created individuals.
6. Repeat steps 3 to 6 (one generation) until the fixed maximal number of generations (stopping criteria) has been reached.

For this GA-optimized WNN model, the number of neurons in the hidden layer of the WNN structure is an important characteristic. In fact, if the number of neurons is insufficient, the network will be unable to approximate the topographic profile. However, if too many neurons are used, overfitting occurs, the model fits the training data extremely well, but it generalizes poorly to new data [22, 23]. Then, we look at studying the evolution of the two defined criteria of the nonlinear GA-WNN

approximation model versus the number of hidden neurons to highlight the relevance of a given mother wavelet function.

3.2 Wavelet library

In this work, an extensive wavelet function library composed by 16 wavelet functions with differing characteristics such as the regularity (the number of vanishing moments), compact support (the speed of convergence to 0), and orthogonality was introduced. Figure 4 shows the shape difference between the wavelet functions of this library.

Note that, in this study, they are considered only mother wavelet functions having explicit formulae because we cannot work out their derivatives.

Their expressions are as follows:

1. Haar wavelet function

It is defined as follows:

$$\Psi(x) = \begin{cases} 1 & if\ 0 \le x < \frac{1}{2} \\ -1 & if\ \frac{1}{2} \le x < 1 \\ 0 & else \end{cases} \tag{5}$$

2. Morlet wavelet function

It is defined by the following equation:

$$\Psi(x) = \cos(1.75x)\exp\left(-\frac{x^2}{2}\right) \tag{6}$$

3. Gaussian wavelet function

It has the following expression:

$$\Psi(x) = \frac{\mathrm{t}}{\sqrt{2\pi}}\exp\left(-\frac{x^2}{2}\right) \tag{7}$$

4. DoG wavelet function

It is the mth order derivative of a Gaussian wavelet where m is a positive integer.

$$\Psi_n(x) = \frac{(-1)^{m+1}}{\sqrt{\Gamma\left(m+\frac{1}{2}\right)}}\frac{d^m}{dx^m}\left(e^{-\frac{x^2}{2}}\right) \tag{8}$$

In this study, we consider three different values of the order parameters m: 1, 3, and 8.

5. Mexican Hat wavelet function

$$\Psi(x) = \frac{2}{\sqrt{3}}\pi^{-0.25}\left(1-x^2\right)\exp\left(-\frac{x^2}{2}\right) \tag{9}$$

The Mexican hat wavelet is an isotropic wavelet family. It is also known as the Ricker wavelet, and it is a special case of the mth order derivative of a Gaussian wavelet with $m = 2$. It is obtained by applying the Laplacian operator to the 2D Gaussian.

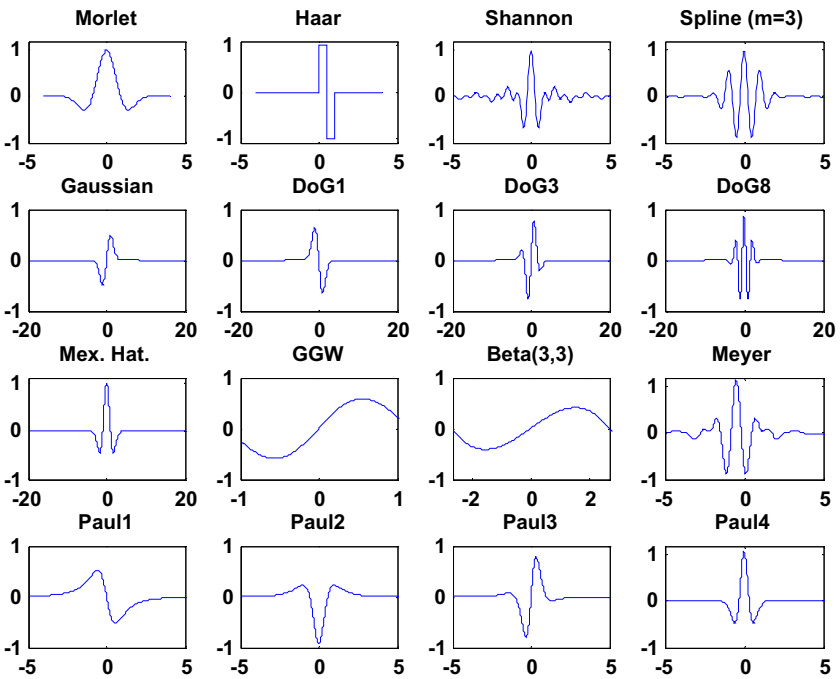

Fig. 4 The "Mother" wavelet function library

6. Shannon wavelet function

It is based on the sinus cardinal function (Eq. 10)

$$\Psi(x) = \frac{\sin\pi(x-0.5) - \sin 2\pi(x-0.5)}{\pi(x-0.5)} \tag{10}$$

7. Meyer wavelet function

It is defined by the following approximate expression:

$$\Psi(x) = 35x^4 - 85x^5 + 70x^6 - 20x^7 \tag{11}$$

8. Spline wavelet function

It is defined by the following expression:

$$\Psi_n(x) = \left(\frac{\sin\left(\frac{\pi x}{m}\right)}{\frac{\pi x}{m}}\right)^m e^{i4\pi^2 x} \tag{12}$$

Cubic spline is considered in this study with $m = 3$.

9. Beta wavelet function

It based on beta function and described by Eq. 13:

$$\Psi_n(x) = \frac{d^{n+1}\beta(x)}{dx^{n+1}} P_{n+1}(x)\beta(x) \tag{13}$$

where
$$P_n(x) = P_{n-1}(x)P_1(x) + P_{n\_1}(x) \quad \forall n > 1 \tag{14}$$

and
$$P_1(x) = \frac{p}{x-x0} - \frac{q}{x1-x} \tag{15}$$

and
$$\beta(x,p,q,x_0,x_1) = \begin{cases} \left(\frac{x-x_0}{x_c-x_0}\right)^p - \left(\frac{x_1-x}{x_1-x_c}\right)^q & \forall x_0 \le x \le x_1 \\ 0 & \text{else} \end{cases} \tag{16}$$

and
$$x_c = \frac{px_1 + qx_0}{p+q} \tag{17}$$

Bellil et al. show [34] that the beta wavelet-based salient point's technique can capture the local feature information, and therefore, they provide a better characterization than Haar or Daubechies wavelets since they are more distinctive and invariant.

10. Paul wavelet function

It has m as an order parameter and is defined by Eq. (18):

$$\Psi(x) = \frac{2^m i^m m!}{\sqrt{\pi}(2m)!}(1-ix)^{-(m+1)} \tag{18}$$

A different value of the order parameter is considered in this study: $m = 1$, 2, 3, and 4.

11. GGW wavelet function

It is not a common wavelet function (Eq. 19). It is developed by authors in [29].

$$\Psi(x) = sin(3x) + sin(0.3x) + sin(0.03x) \tag{19}$$

4 Identification of relevant wavelet function for multiscale characterization of abraded surfaces

The relevance of the considered wavelet functions for dealing with the quality of the reconstruction of the topographic profile of abraded surfaces and the detection of its features was investigated.

4.1 Wavelet function classification

In this study, topographic profiles of abraded surfaces by six different abrasive finishing processes (turning, face milling, milling, grinding, honing, and polishing) are considered. For each abrasive process, the input topographic data are composed by 40 profiles generated under various operating conditions. Overall, 30 of each dataset (75%) were used in the training phase and 10 profiles (25%) were used in the validation phase of each model. All the surface micro-profiles are acquired perpendicularly to the machining direction by using a 2D Surfscan stylus profilometer. This device consists of a diamond tip with a 2-μm rounded-end radius and has a 10-nm vertical resolution. Each recorded profile consists of 2405 points that are equally spaced by 2-μm distance.

For each wavelet function from the library, WNN models were trained and validated by varying the imposed number of hidden neurons from 4 to 64 neurons. The number of hidden neurons corresponds to the number of scaled and translated wavelets, that is, to the level of decomposition. The parameters of the GA and WNN algorithm for each simulation are shown in Table 1. A measure of the quality of each resulted approximation model is then computed by using the mean square error and correlation criteria.

Results of the evolution of MSE function of the number of hidden neurons show that the considered wavelet functions of this library can be classified into three groups:

1. *Group 1 (nonadapted wavelet):* This first group is composed by beta, Meyer, and Shannon wavelet functions. It does not permit to establish a valuable model of the multiscale decomposition while even varying the number of wavelet hidden neurons. In this case, the MSE error reaches high values and correlation criterion r is low (< 0.7). It can also be remarked that MSE and correlation

Table 1 The parameters of the GA and WNN algorithm for each simulation

GA parameters	
Population size	30
Number of generations	80
Number of individuals in each tournament selection	5
Ranking selection method	Normalized geometric distribution [33]
Crossover method	Arithmetic crossover by linear interpolation [33]
Mutation method	Multi-nonuniform mutation [33]
Number of trials	10
WNN architecture and training parameters	
The number of layers	3
The number of neurons on the layers	Input: data vector size
	Hidden: 4; 16; 64
	Output: data vector size
The initial weights and biases	Random values
Learning rule	Back-propagation
Training rate	0.001
Momentum coefficient	0.95
Number of epochs	300

criteria vary randomly with the increases in the number of scaled wavelet functions (hidden neuron). Tables 2 and 3 resume, respectively, MSE and correlation criteria of the

Table 2 MSE criteria of the approximating model using the first group of wavelet functions

Abrasion process	Number	Beta	Meyer	Shannon
Milling	4	2.81E−03	1.30E+147	1.59E−02
	16	1.79E+05	2.70E+154	1.50E−02
	64	1.54E+154	5.40E+188	9.27E+03
Face milling	4	1.05E+01	1.50E+132	2.03E−02
	16	8.52E−03	3.70E+122	1.54E−02
	64	2.00E+145	2.40E+152	3.06E+01
Honing	4	1.05E+01	1.20E+92	1.29E−02
	16	8.53E−03	6.70E+103	1.48E−02
	64	2.00E+145	3.40E+138	5.31E+31
Grinding	4	1.45E+04	3.05E+141	2.03E−02
	16	5.64E−01	1.25E+149	2.02E−02
	64	2.41E+150	4.40E+142	1.74E+05
Turning	4	1.17E+04	9.04E+142	1.63E−02
	16	2.03E+08	1.57E+147	2.02E−03
	64	1.24E+149	3.76E+141	1.60E+17
Polishing	4	1.09E−02	4.26E+142	1.97E−02
	16	1.17E+01	4.98E+145	2.37E−02
	64	1.99E+148	6.13E+136	1.91E−01

Table 3 Correlation criteria of the approximating model using the first group of wavelet functions

Abrasion process	Number	Beta	Meyer	Shannon
Milling	4	1.00	0.01	0.24
	16	0.14	0.03	0.47
	64	0.04	0.07	0.07
Face milling	4	0.02	0.01	0.08
	16	0.02	0.02	0.70
	64	0.02	0.07	0.87
Honing	4	−0.98	0.02	0.66
	16	−0.97	0.05	0.39
	64	−0.96	0.09	0.04
Grinding	4	1.00	0.02	0.10
	16	0.97	0.04	0.13
	64	0.99	0.09	0.07
Turning	4	1.00	0.04	0.04
	16	0.12	0.10	0.99
	64	0.33	0.14	−0.03
Polishing	4	1.00	0.03	0.70
	16	0.90	0.09	−0.87
	64	0.89	0.12	0.08

model's performances by using wavelets belonging to this group for the topographic data of different abrasive processes and by using 4, 16, or 64 hidden neurons. Then, we can conclude that wavelet functions of this group do not allow to describe features of abraded topographic profiles.

2. *Group 2 (nonrelevant wavelet):* This group of wavelet function allows during the validation step of the trained model to obtain an output signal correlated to the input topographic signal ($r > 0.85$) for all the studied abraded surfaces. However, they present a random performance behavior or any amelioration (reduction) in terms of mean square error criteria when varying the number of scaled and translated wavelets that compose the model (Fig. 5). Then, we can conclude that wavelet functions of this group are not well adapted to properly analyze abraded topographic profiles. We find the eight derivatives of Gaussian (DoG8) and spline wavelet function belonging to this group for all the considered abrasive processes (Fig. 5).
3. *Group 3 (adapted wavelet):* The third category of wavelet function allows developing a model that has the considerable capability to be applied with satisfactory accuracy. In fact, correlation criteria are always greater than 0.97 by using 4, 16, or 64 hidden neurons in the GA-WNN structure. Moreover, the MSE error decreases systematically with each addition of novel wavelet neurons in the WNN structure. Further, it reaches an acceptable value for most of this wavelet function category by using only almost 16 hidden neurons (Fig. 6).

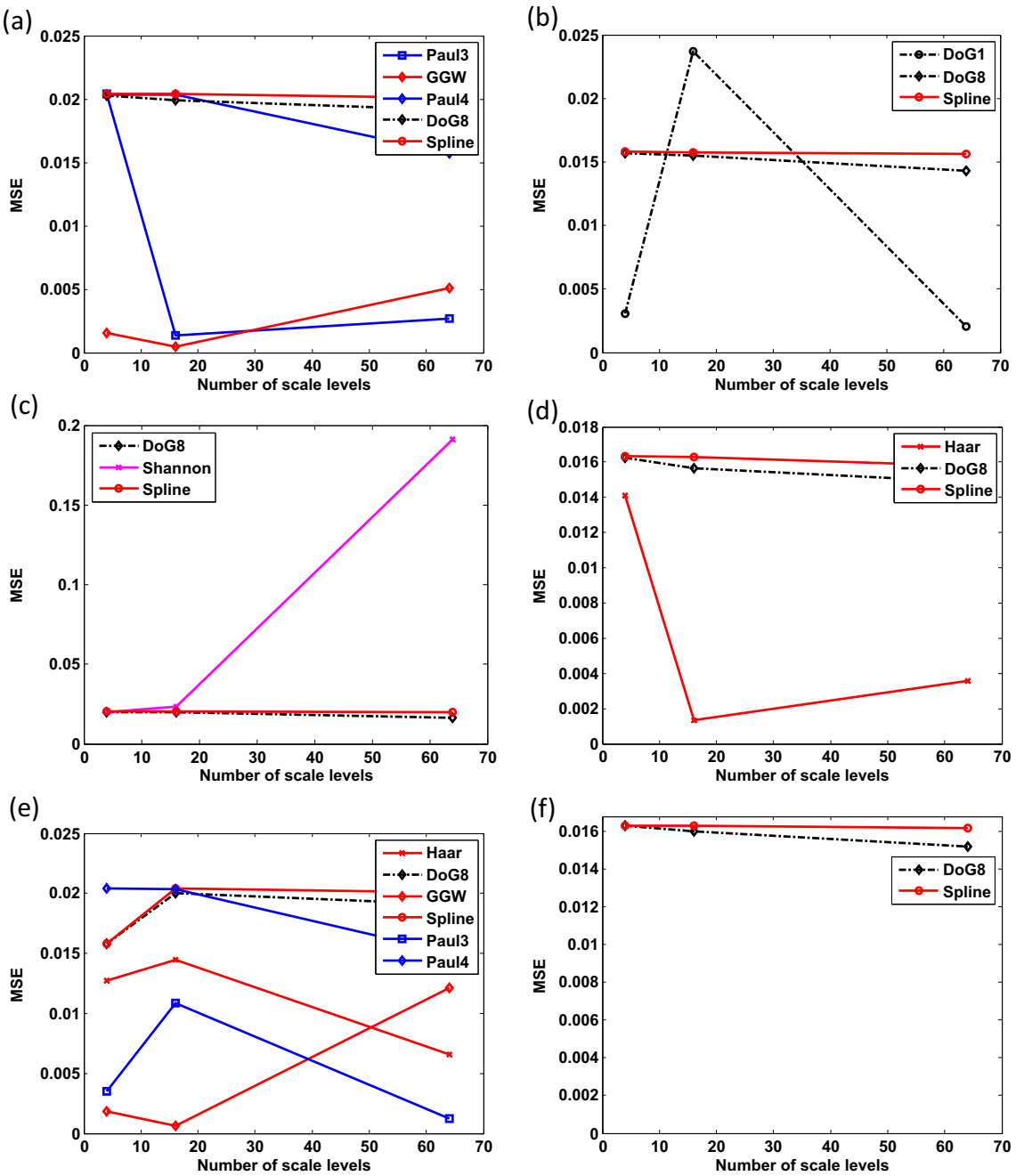

Fig. 5 Mean square errors of the approximating model using the second category of wavelet functions for finished surfaces with different abrasive processes, respectively. **a** Grinding. **b** Honing. **c** Polishing. **d** Milling. **e** Face milling. **f** Turning

A ranking of the relevance of wavelet functions of the third group can be addressed by comparing the MSE evolution with the hidden neuron number. The most relevant wavelet function from this category is the one that leads to the more reduced MSE using less hidden neurons. Based on this classification condition, we can draw the conclusion that the Gaussian wavelet and its derivative are the more relevant wavelet functions for the characterization of surfaces generated by abrasive processes (Fig. 6) than Morlet and Paul wavelets.

Further, inside the Gaussian wavelet and its derivatives, we found that the first derivative of the Gaussian wavelet function (DoG1) leads to the lower MSE for all the abrasive processes (Fig. 7); then, it is more appropriate and can be considered a universal wavelet adapted to the analysis of abraded surface textures.

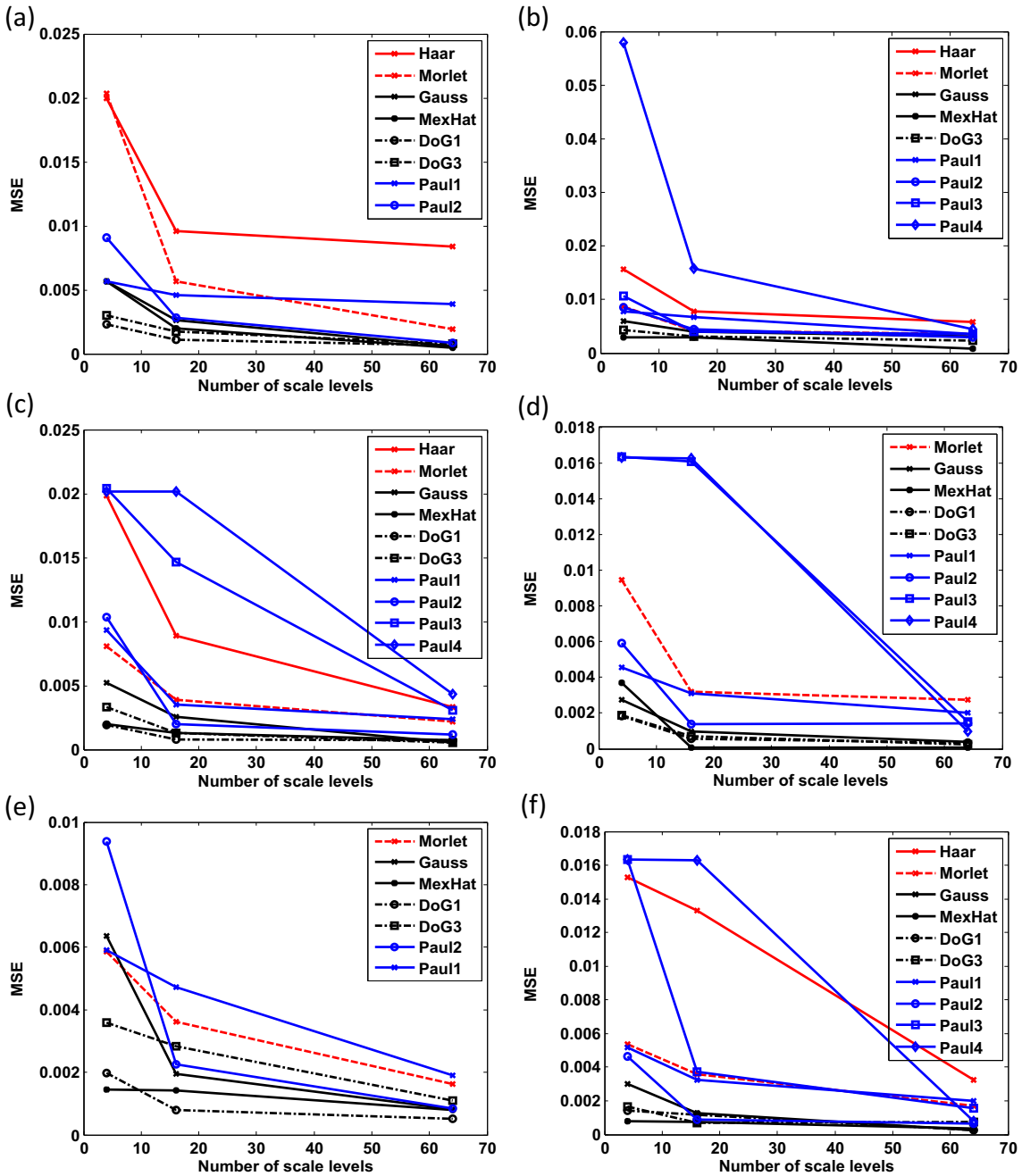

Fig. 6 Mean square errors of the approximating model using the third category of wavelet functions for finished surfaces with different abrasive processes, respectively. **a** Grinding. **b** Honing. **c** Polishing. **d** Milling. **e** Face milling. **f** Turning

Two widespread criteria were commonly used by researchers to determine qualitatively the suitability of a wavelet function for a given application which are as follows:

1. The wavelet function properties such as

   - *Symmetry:* If the wavelets are not symmetric, then the wavelet transform of the mirror of an image is not the mirror of the wavelet transform.
   - *Smoothness*: This property is determined by the number of vanishing moments. If the wavelet has *N* vanishing moments, the wavelet transform can be interpreted as a multiscale differential operator of order *N*. This yields a first relation between the differentiability of the analyzed signal and its wavelet transform decay at fine scales.
   - *Orthogonality*: This property can be too restrictive at times.
   - *Compact support*: This property is a function of the filter length.

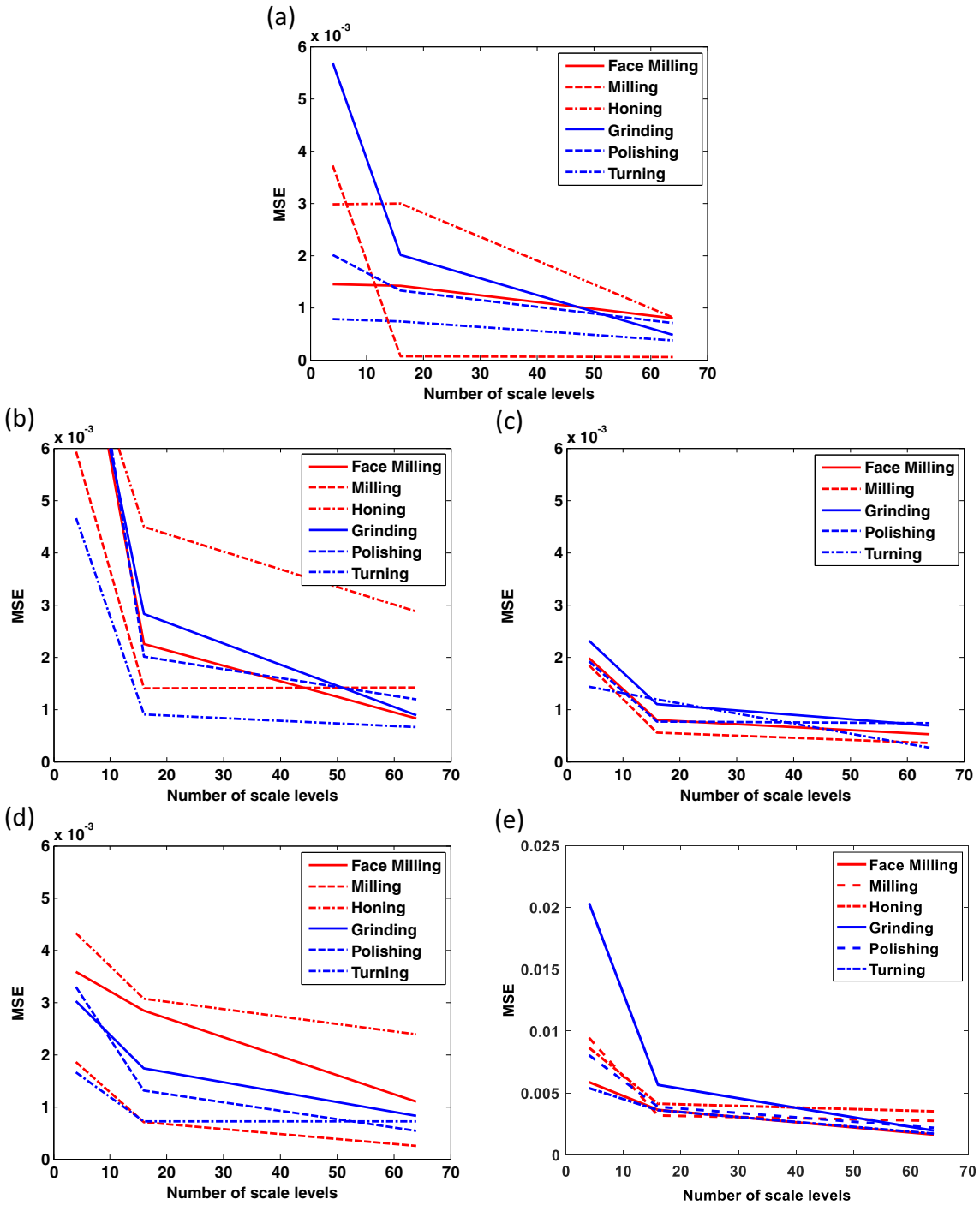

Fig. 7 Mean square errors of the approximating model of different finished surfaces with different abrasive processes, respectively, using **a** MexHat, **b** Paul2, **c** Dog1, **d** Dog3, and **e** Morlet wavelet function

2. The matching between the shape of profile features and the one of the wavelet function.

In the two next sections, results of the proposed approach are then compared to those resulting from these two qualitative methods.

4.2 Influence of wavelet properties on wavelet function relevance

Table 4 summarizes the principal properties of the library wavelet functions used in this study, and the identified wavelet function pertinence using the proposed selection approach.

Table 4 Wavelet functions properties and its determined relevance

Wavelet families	Properties					Relevance
	Real/Complex	Orthogonal	Compact support	Symmetry	Regularity	
Meyer	Real	Yes	No	Yes	Infinitely differentiable	–
Shannon	Real	Yes	No	Yes	Infinitely differentiable	–
Beta (3,3)	Real	Yes	Yes	Yes	Infinitely differentiable	–
Spline (order = 3)	Complex	Yes	No	Yes	Infinitely differentiable	o
Dog (*N*)	Real	No	Yes	Yes	Number of the derivative (*N*)	o (*N* = 8) ++ (*N* = 1;3)
Mexican Hat	Real	No	No	Yes	2	+
Gaussian	Real	No	No	Yes	1	+
Haar	Real	Yes	Yes	Yes	Discontinuous	o/+
Morlet	Real	No	No	Yes	Infinitely differentiable	+
Paul (order = m)	Complex	No	No	Yes	Infinitely differentiable	+
GGW	Real	No	No	Yes	Infinitely differentiable	−/o

– Group 1 (not adapted wavelet), *o* group 2 (not relevant wavelet), + group 3 (relevant wavelet)

We can conclude clearly from Table 4 that relevant wavelets do not require specific properties to decide on its suitability for multiscale characterization of an abraded surface. Indeed, no rule can be established to justify the wavelet function choice.

4.3 Influence of wavelet shape and decomposition levels on wavelet function relevance

The topographic profile of the abraded surface can be seen as the superposition of a unique elementary pattern that physically represents the footprint of the elementary mechanical process that creates the abrasion of the surface [18, 19] (Fig. 8).

Shape matching between wavelet base function and analyzed profile features has been considered as an alternative approach to wavelet function selection. In fact, it is well known that wavelet analysis is a measure of the correlation between surface features and the wavelet shape at different positions and scales of the analyzed signal, and therefore, the signal reconstruction and statistical estimators are strongly influenced by the wavelet shape. However, it is generally difficult to accurately match the shape of a signal to that of a base wavelet through a visual comparison.

It can be remarked that the major nonadapted wavelet functions (group 1 and group 2) have a different shape from this main elementary pattern of abraded surfaces (Figs. 4 and 8). However, wavelet functions belonging to group 3 (relevant wavelet) have a shape with single oscillation similarly to the abraded surface pattern. In particular, the DoG1 wavelet function was found to be more relevant than the Paul2 wavelet function, although this latter has a more similar shape to the elementary main pattern. This can be explained by the fact that the shape of the optimal wavelet DoG1 reproduces only one ridge of the elementary abrasion pattern. In consequence, the elementary abrasion pattern is entirely approximated not only by a one-scaled and translated wavelet but by a two-scaled and translated DoG1 wavelet. This then permits a better adaption to the abrasion pattern and especially allows a better approximation of prospective nonsymmetric ridges surrounding a groove.

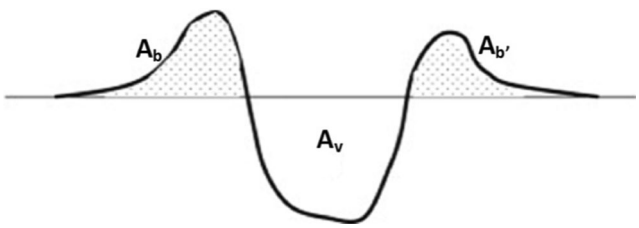

Fig. 8 Schematic representation of groove and ridge profiles generated by individual abrasive grit [19]

We can also remark that although the Haar wavelet is not a continuous function and therefore introduces discontinuity into the decomposed profile, it appears in the group of adapted wavelet function (group 3) for practically all the abrasive processes (Fig. 6). This can be explained by its shape presenting only one oscillation like the other wavelet functions of this group and its capacity to adapt to sharp features such as steps and grooves.

It can be concluded that classification of the relevance of an analysis wavelet function is not based only on its shape but also on its capacity to properly replicate surface features and that the proposed approach allows an objective qualification of wavelet function relevance.

Otherwise, it can be observed that the influence of the shape of the wavelet function can be greatly reduced by increasing the number of decomposition level (Figs. 6 and 7), but it is obvious that, in this case, the representation of surface features will became sparse and each pertinent information will be diluted between several wavelet scales and spatial

positions, thus making it difficult to properly detect all the textural characteristics.

5 Conclusions

A novel method for the classification of wavelet function relevance for multiscale surface topography characterization was proposed. It consists of tracking the performance of nonlinear regression models of the multiscale wavelet decomposition based on the genetic algorithm-optimized wavelet neural network by varying the number of hidden neurons. It was successively applied to the identification of relevant wavelet function for multiscale characterization of various abrasive finishing processes. Considering a wavelet library composed by 16 different wavelet basis functions, results show that Gaussian and its derivative wavelet functions are the more relevant and particularly the first derivative (DoG1) is the most relevant to highlight the multiscale patterns of abraded surfaces. Further, it demonstrated that increasing the decomposition level can reduce the impact of the wavelet function choice.

References

1. Nouioua M, Yallese MA, Khettabi R, Bouhalais ML, Girardin F (2017) *Investigation of the performance of the MQL, dry, and wet turning by response surface methodology (RSM) and artificial neural network (ANN)*. Int J Adv Manuf Technol 93:2485–2504
2. Ununе DR, Mali HS (2016) *Artificial neural network-based and response surface methodology-based predictive models for material removal rate and surface roughness during electro-discharge diamond grinding of Inconel 718*. Proc Inst Mech Eng B 230(11): 2081–2091
3. Homami RM, Tehrani AF, Mirzadeh H, Movahedi B, Azimifar F (2014) *Optimization of turning process using artificial intelligence technology*. Int J Adv Manuf Technol 70(5–8):1205–1217
4. Wen L, Li X, Gao L, Yi W (2016) *Surface roughness prediction in end milling by using predicted point oriented local linear estimation method*. Int J Adv Manuf Technol 84(9–12):2523–2535
5. Vahabli E, Rahmati S (2016) Application of an RBF neural network for FDM parts' surface roughness prediction for enhancing surface quality. Int J Precis Eng Manuf 17(12):1589–1603
6. Samtas G (2014) *Measurement and evaluation of surface roughness based on optic system using image processing and artificial neural network*. Int J Adv Manuf Technol 73(1–4):353–364
7. Ventaka RK, Vidhu KP, Anup KT, Narayana RN, Murthy PBGSN, Balaji M (2016) *An artificial neural network approach to investigate surface roughness and vibration of workpiece in boring of AISI1040 steels*. Int J Adv Manuf Technol 83(5–8):919–927
8. Whitehouse DJ (1993) A philosophy of linking manufacture to function—an example in optics. Proc Inst Mech Eng B J Eng Manuf 207(1):31–42
9. Mezghani S, El Mansori M, Massaq A, Ghidossi P (2008) Correlation between surface topography and tribological mechanisms of the belt-finishing process using multiscale finishing process signature. C R Mécanique 336(10):794–799
10. Le Goïc G, Bigerelle M, Samper S, Favrelière H, Pillet M (2016) *Multiscale roughness analysis of engineering surfaces: a comparison of methods for the investigation of functional correlations*. Mech Syst Signal Process 66:437–457
11. Khawaja Z, Guillemot G, Mazeran P-E, El Mansori M, Bigerelle M (2011) Wavelet theory and belt finishing process, influence of wavelet shape on the surface roughness parameter values. J Phys Conf Ser 311:012013
12. Jiang X, Scott P, Whitehouse D (2008) Wavelets and their applications for surface metrology. CIRP Ann Manuf Technol 57(1):555–558
13. Serpin K, Mezghani S, El Mansori M (2015) Multiscale assessment of structured coated abrasive grits in belt finishing process. Wear 332:780–787
14. Bigerelle M, Giljean S, Mathia TG (2011) Multiscale characteristic lengths of abraded surfaces: three stages of the grit-size effect. Tribol Int 44:63–80
15. Van Gorp A, Bigerelle M, Grellier A, Iost A, Najjar D (2007) A multi-scale approach of roughness measurements: evaluation of the relevant scale. Mater Sci Eng C 27(5–8):1434–1438
16. Goic GL, Favreliere H, Samper S, Formosa F (2011) Multiscale modal decomposition of primary form, waviness and roughness of surfaces. Scanning 33(5):332–341
17. Mallat S (1989) A theory for multiresolution signal decomposition: the wavelet representation. IEEE Pattern Anal Mach Intell 11(7): 674–693
18. Mezghani S, Sabri L, El Mansori M, Zahouani H (2011) On the optimal choice of wavelet function for multiscale honed surface characterization. J Phys Conf Ser 311(1):012025
19. Bigerelle M, Guillemot G, Khawaja Z, El Mansori M, Antoni J (2013) *Relevance of Wavelet Shape Selection in a complex signal*. Mech Syst Signal Process 41(1–2):14–33
20. Ahuja N, Lertrattanapanich S, Bose K (2009) *Properties determining choice of mother wavelet*. IEE Proc Vision Image Signal Proc 152:659–664
21. Billings SA, Wei H-L (2005) A new class of wavelet networks for nonlinear system identification. IEEE Trans Neural Netw 16(4): 862–874
22. Zhang Q, Benveniste A (1992) Wavelet networks. IEEE Trans Neural Netw 3(6):889–898
23. Alexandridis A, Zapranis A (2013) *Wavelet neural networks: a practical guide Neural Networks*. Neural Netw 42:1–27
24. Mezghani S, Zahouani H, Piezanowski JJ (2011) Multiscale characterizations of painted surface appearance by continuous wavelet transform. J Mater Process Technol 211(2):205–211
25. Zahouani H, Mezghani S, Vargiolu R, Dursapt M (2008) *Identification of manufacturing signature by 2D wavelet decomposition*. Wear 264(5):480–485
26. Torrence C, Compo GP (1998) A *practical guide to wavelet analysis*. Bull Am Meteorol Soc 79(1):61–78
27. Awad M (2014) Using genetic algorithms to optimize wavelet neural networks parameters for function approximation. Int J Comput Sci Issues 11(1):256–257
28. Feng L, Jianhua X, Zhanyong W (2009) *Application of GA optimized wavelet neural networks for carrying capacity of water resources prediction*. Environ Sci Inf Appl Technol ESIAT 1:308–311. https://doi.org/10.1109/ESIAT.2009.59
29. Wang G, Guo L, Duan H (2013) Wavelet neural network using multiple wavelet functions in target threat assessment. Sci World J 2013:632437 7 pages
30. Wang SF, Li C, Xie XQ, Wang J (2014) *Application research of WNN optimized by GA in VRLA battery degradation prediction*. Appl Mech Mater 664–650:2087–2091 Machine tool technology and mechatronics engineering by Trans Tech Publications, Pfaffikon, Switzerland; 2014

31. Anijdan SHM, Bahrami A, Hosseini HRM, Shafyei A (2006) *Using genetic algorithm and artificial neural network analyses to design an Al-Si casting alloy of minimum porosity.* Mater Des 27(7):605–609
32. Khalick MAE, Hong J, Wang D (2017) *Polishing of uneven surfaces using industrial robots based on neural network and genetic algorithm*. Int J Adv Manuf Technol 93(1–4):1463–1472
33. Houck CR, Joines JA, Kay MG (1995) A genetic algorithm for function optimization: A Matlab implementation, Technical Report NCSU-IE-TR-95-09, North Carolina State University, Raleigh, NC
34. Bellil W, Ben AC, Alimi A (2006) *Synthesis of wavelet filters using wavelet neural networks*. World Acad Sci Eng Technol 13:108–111